JACS
JOURNAL OF THE AMERICAN CHEMICAL SOCIETY

ARTICLE

pubs.acs.org/JACS

Autocatalysis and Surface Catalysis in the Reduction of Imines by SmI_2

Chintada Nageswara Rao and Shmaryahu Hoz*

Department of Chemistry, Bar-Ilan University, Ramat-Gan 52900, Israel

Supporting Information

ABSTRACT: The reduction of the three imines, *N*-benzylidene aniline (**BAI**), *N*-benzylidenemethylamine (**BMI**), and benzophenone imine (**BPI**), with SmI_2 gives the reduced as well as coupled products. The reactions were found to be autocatalytic due to the formation of the trivalent samarium in the course of the reaction. When preprepared SmI_3 was added to the reaction mixture, the reaction rate increased significantly. However, the kinetics were found to be of zero order in SmI_2. This type of behavior is typical of surface catalysis with saturation of the catalytic sites. Although no solids are visible to the naked eye, the existence of microcrystals was proven by light microscopy as well as by dynamic light scattering analysis. Although HRTEM shows the existence of quantum dots in the solid, we were unable to make a direct connection between the existence of the quantum dots and the catalytic phenomenon. In the uncatalyzed reaction, the order of reactivity is **BPI** > **BMI** > **BAI**. This order does not conform to the electron affinity order of the substrates but rather to the nitrogen lone pair accessibility for complexation. This conclusion was further supported by using HMPA as a diagnostic probe for the existence of an inner sphere electron transfer reaction.

INTRODUCTION

SmI_2 was discovered by Matignon and Caze in 1906[1a] and was reintroduced ca. 70 years later, in 1977, to the chemical community by Kagan's group, becoming one of the most popular reducing agents.[1b] Among its many advantages are that reductions could be carried out under homogeneous conditions, that it is a mild agent, and that its reactivity can be tuned by various additives.[2] Under normal conditions, it reacts satisfactorily with low lying LUMO compounds, such as those we have studied in the past, that is, those possessing activated carbon−carbon double bonds[3] or carbonyl functions.[4] The reactions of these two families of compounds differed significantly from each other. In this Article, we report on the SmI_2 reduction of a third type of double bond, that of an imine. It appears that this carbon−nitrogen double bond displays chemistry, which differs markedly, not only from that of activated olefins and carbonyl compounds, but also, to the best of our knowledge, from the chemistry reported to date for SmI_2 reactions in general.

Reactions of imines with SmI_2 are well documented in the literature.[5] In general, depending on conditions, two types of reactions are observed, reduction to amines and coupling (eq 1).[5j]

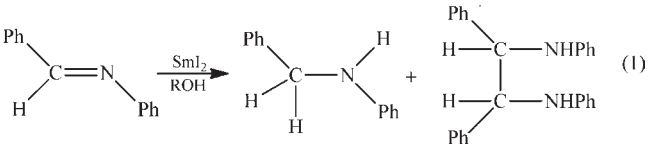

(1)

We originally focused our studies on *N*-benzylidene aniline (**BAI**). However, in light of the surprising results, and to examine their generality, we extended the investigation to *N*-benzylidenemethylamine (**BMI**) and benzophenone imine (**BPI**).

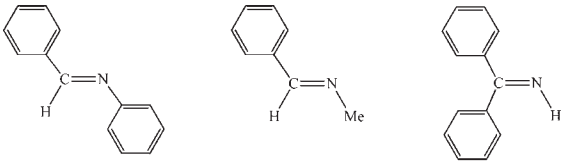

BAI **BMI** **BPI**

RESULTS AND DISCUSSION

The reactions of **BAI** were followed using a stopped-flow spectrometer. The kinetics was monitored by following the disappearance of the absorption of SmI_2 at 619 nm. Figure 1 shows the kinetic trace obtained under pseudo first-order conditions (excess imine) in the presence of 1 M MeOH.

As can be seen, the reaction is autocatalytic. The slopes in abs/s units at 1 s time intervals are given in Table 1.

The rate first goes up and then toward the end of the reaction decreases, demonstrating an autocatalytic process.[6] This autocatalytic behavior repeated itself for all of the methanol concentrations examined in the range 0.1−4 M. We have also noticed that the concentration of MeOH did not have a significant effect on the reaction rate. For example, in one case where the MeOH concentration was varied by a factor of 40 (from 0.1 to 4 M), the initial rate varied by a factor of 3 only. In addition, the reproducibility of the measurements was not very good. Because we have found in the past that MeOH coordinates efficiently to SmI_2,[3a,e] an

Received: June 24, 2011
Published: August 17, 2011

dx.doi.org/10.1021/ja205885q | *J. Am. Chem. Soc.* 2011, 133, 14795–14803

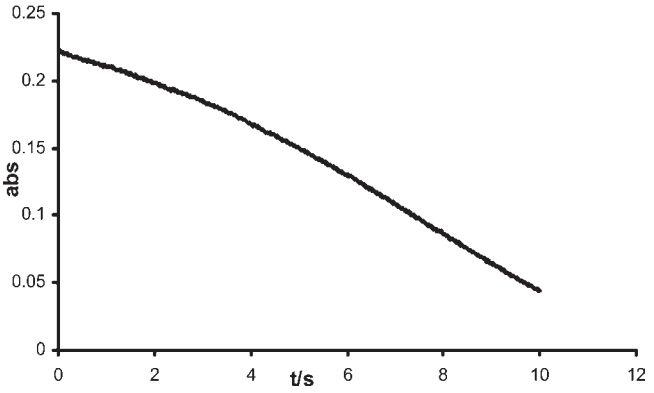

Figure 1. The kinetic trace for the reaction of **BAI** 25 mM, SmI_2 2.5 mM, and MeOH 1 M in THF.

Table 1. Slopes for the Kinetic Trace of Figure [1]

t/s	slope/−abs s^{-1}	t/s	slope/−abs s^{-1}
0	0.011	5	0.020
1	0.0126	6	0.0218
2	0.0132	7	0.0223
3	0.0165	8	0.0218
4	0.0179	9	0.0207

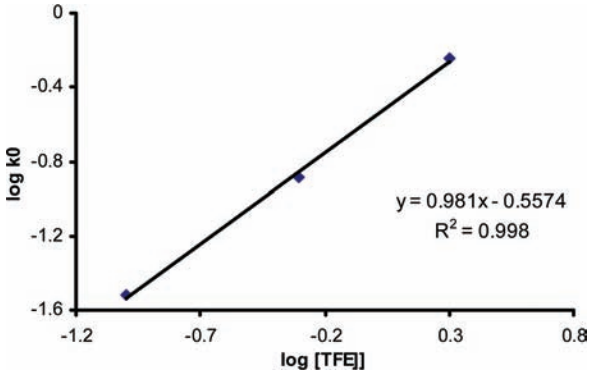

Figure 2. A plot of the log initial slopes (k_0) versus log[TFE] in the reaction of 1 mM SmI_2 and 12.5 mM **BAI**.

observation that has been confirmed many times since then,[2] we have gone over to the use of trifluoroethanol (TFE), a proton donor that does not form complexes with SmI_2.

The reactions in the presence of TFE presented the same autocatalytic behavior. However, a variation of the concentration of the proton donor over the range 0.2−2 M using initial rates showed a first order in TFE (Figure 2).

Thus, the autocatalytic behavior is independent of the complexation ability or of the nature of the proton donor.

Next, we determined the kinetic order in the imine. This was done in two concentration ranges, where the imine is in large excess and where the SmI_2 is in large excess, both under pseudo first-order conditions. At high imine concentrations, we varied the imine concentration and measured the initial slope of the kinetic trace (k_0). The data are presented in Figure 3, showing first-order kinetics in the imine.

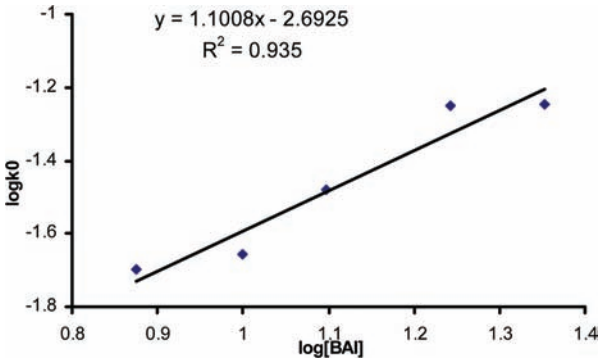

Figure 3. A plot of log k_0 versus log[**BAI**] showing first-order kinetics.

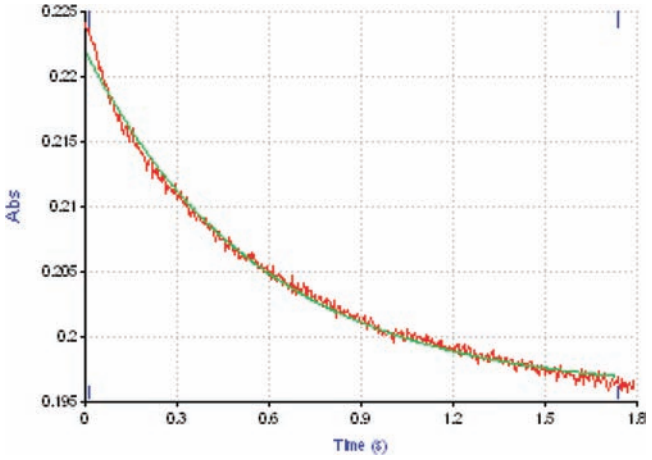

Figure 4. Kinetic trace and a fit to a first-order analysis in the reaction of **BAI** (0.25 mM), SmI_2 (2.5 mM), k = 1.8 s^{-1}.

In the lower imine concentration range, we reduced the concentration of the **BAI** by 50−100 fold, and the concentration of the SmI_2 remained as before. In this case, the disappearance of SmI_2 reflects the disappearance of the imine. Figure 4 shows such a kinetic trace with a very good fit to a first order. Thus, the kinetic order in the imine in both concentration ranges is one.

Autocatalysis is usually observed when one of the reaction products catalyzes the reaction. The most reasonable candidate in this case is Sm^{3+}, which is produced as a result of the electron transfer from SmI_2. Sm^{3+} can complex to the imine and increase its electrophilicity, thereby enhancing the rate of the electron transfer step relative to the uncoordinated imine. A simple test to verify the existence of such a catalysis would be to add externally prepared SmI_3. In this case, one would expect that if the initial reaction mixture already contains a significant amount of the catalyst, the autocatalytic behavior will be significantly reduced and the reaction rate will decrease with time as the reaction progresses, due to the depletion of the reactants in a manner typical of first or second order kinetics. In a series of experiments in the presence of 0.1−2 M TFE, 1.25 mM SmI_2, and various concentrations of SmI_3, it was found that the addition of SmI_3 indeed enhanced the reaction rates. However, the kinetic trace, as shown in Figure 5, was a typical zero-order plot. Following the absorption of SmI_2, a constant rate (slope) was obtained from the beginning to nearly the end of the reaction. It should be emphasized that zero-order reactions were also obtained with

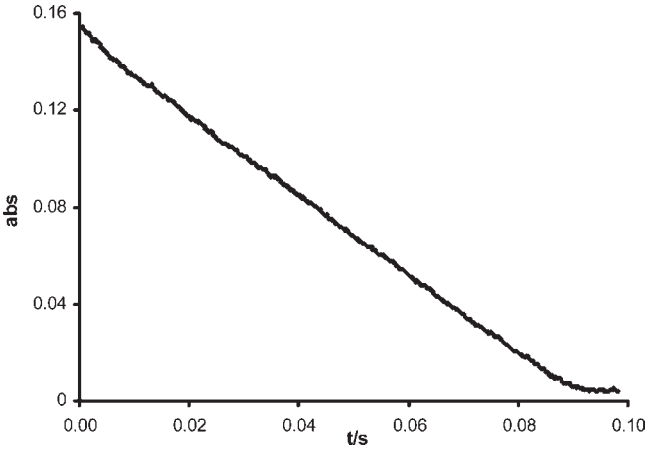

Figure 5. The kinetic trace (abs vs *t*) in the reaction of **BAI** 12.5 mM, SmI_2 1.25 mM, SmI_3 1.25 mM, and TFE 0.1 M.

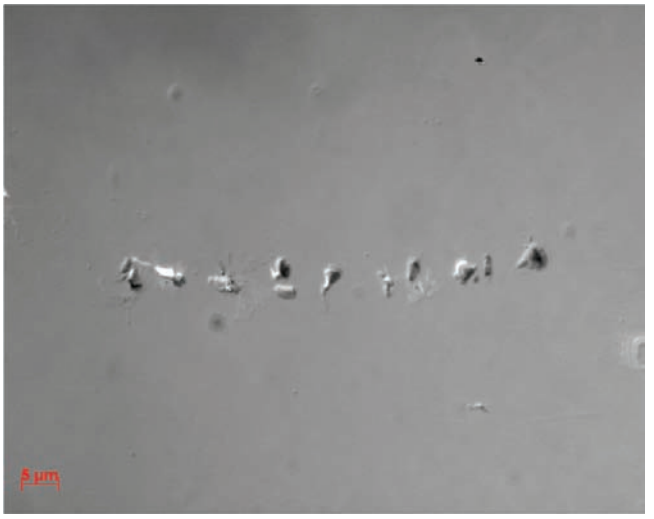

Figure 6. SmI_3 microcrystals using light microscopy.

various concentrations of MeOH as the proton donor (see the Supporting Information).

Zero-order kinetics is typical of a saturation phenomenon. The classical example is an enzymatic reaction where the catalytic site is saturated. In this case, because the rate is determined by the output of the catalytic site, which is fully saturated, increasing the concentration of the reactants does not increase the rate. In the present case, the place of the enzyme may be taken by a catalytic site on a surface. We know that SmI_3 is relatively insoluble in THF. However, at the concentrations used, the solutions seem clear to the naked eye. We, therefore, conducted two types of experiments to see whether, despite the fact that the reaction mixtures were clear, they might contain solids (microcrystals). The first experiment was dynamic light scattering (DLS), and the second was light microscopy. The DLS measurements were carried out on SmI_3 prepared from SmI_2 and I_2 as well as on a typical reaction mixture (**BAI**, 12.5 mM; SmI_2, 1.25 mM; and TFE, 0.1 M). The measurements were performed ca. 10 min after the preparation of the samples (10 min is the time needed to transfer the sample from the glovebox to the DLS instrument). Although the solutions remained clear to the naked eye, particles

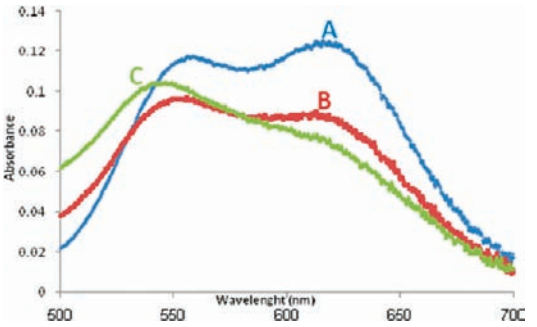

Figure 7. UV spectra of SmI_2–HMPA complex in THF solution. SmI_2 = 1.25 mM; [HMPA]: A = 0.0 mM, B = 2.0 mM, and C = 4.0 mM.

ranging from 2 to 250 nm were observed. The size of these particles grew with time, probably due to aggregation (see the Supporting Information).The light microscopy study also showed the existence of particles in the solution with fluorescence typical of the lanthanides (Figure 6 and the Supporting Information).

HRTEM analysis showed the existence of quantum dots (see the Supporting Information), which may be responsible for the surface catalysis. The above analyses clearly show that, although the solutions seem to be clear, they actually contain microcrystals, and thus support our hypothesis regarding the existence of catalytic sites on solid SmI_3. Because the amount of solid SmI_3 is similar to the concentration of SmI_2 and the imine, it is clear that the kinetics of the formation of the microcrystals and their size, as well as shape and size distribution, may vary from one experiment to the other. Therefore, it is not surprising that the reproducibility of the rate constant was not very good.

We now turn to a powerful mechanistic diagnostic tool, HMPA. This ligand is known to strongly coordinate to SmI_2 and significantly increase its reduction potential.[7] However, being a "hard" ligand, we assumed that it would coordinate more strongly to Sm^{3+}, which is harder than Sm^{2+}. To examine our hypothesis, we performed the following experiment whose results are depicted in Figure 7. Figure 7 shows the spectra of SmI_2 1.25 mM, after the addition of 2 mM and after the addition of 4 mM HMPA. The ratio of the heights of the two peaks in the solution of SmI_2 itself is 1.05 with the longer wavelength peak higher than the other. The addition of 2 mM HMPA changes this ratio to 0.994, with the shorter wavelength peak having a higher absorbance. After the addition of 2 more mM of HMPA, the shape of the spectrum changes and the longer wavelength absorption turns into a shoulder. The ratio of the absorbance at the original two wavelengths is now 0.734.

The addition of 1.25 mM of Sm^{3+} restored completely, in both cases, the original shape of the SmI_2 spectrum with the peak ratios of 1.053 and 1.067, respectively. This clearly indicates that the affinity of HMPA to SmI_3 is significantly larger than that to SmI_2. Therefore, the addition of HMPA will slow the catalytic reaction, and as its concentration increases, the appearance of the autocatalytic behavior will be delayed until enough "free" Sm^{3+} will have accumulated to form microcrystals. Eventually, when the concentration of HMPA is large enough, there will be no microcrystals present in the solution and the autocatalytic behavior will disappear. At this point, the reaction should display a "normal" kinetics. Figure 8 shows the kinetic traces for the reaction of **BAI** at various concentrations of HMPA.[8]

It is clearly seen that the onset of the catalytic stage (the fast drop in the OD, which takes place within the first half second) is

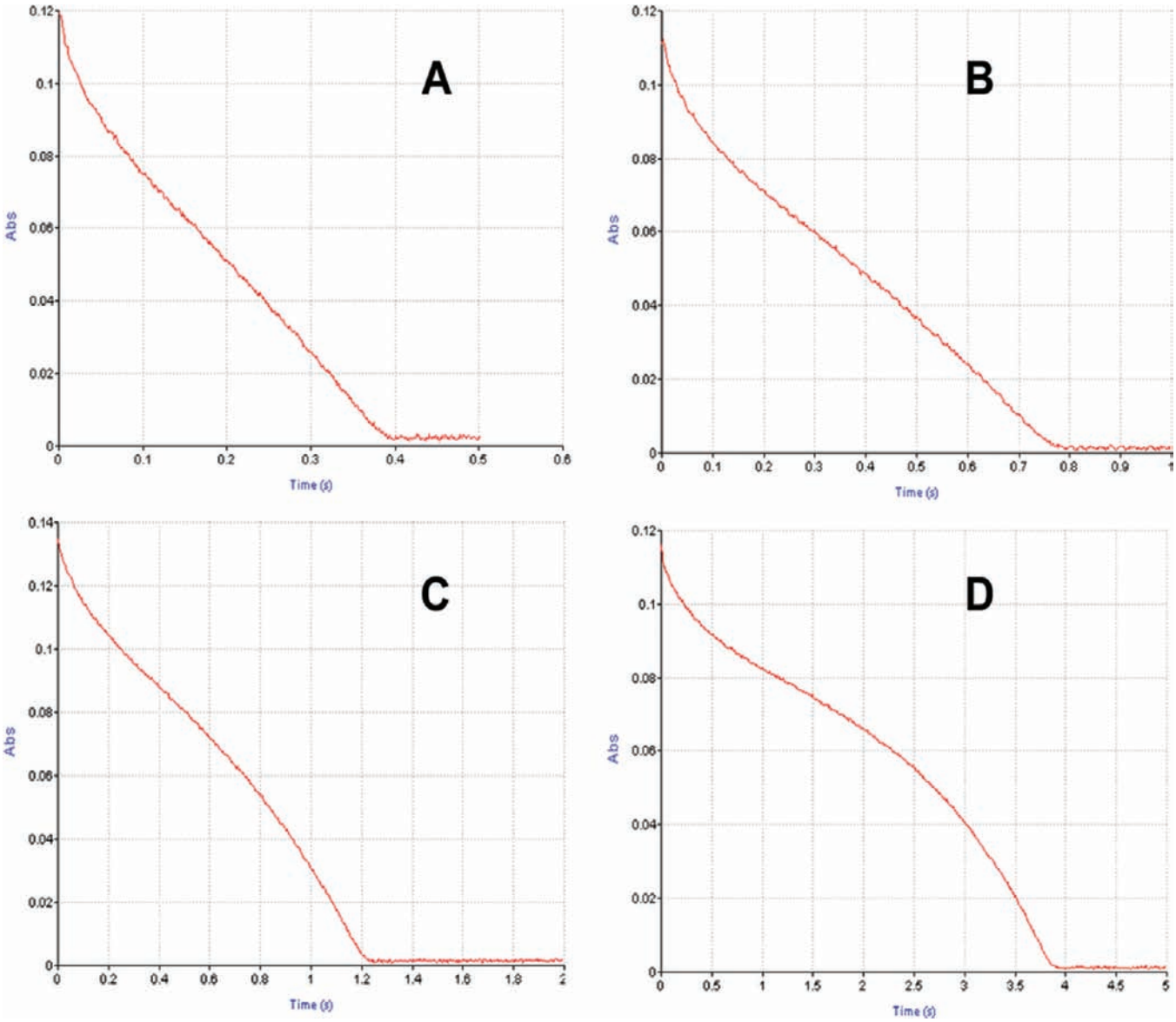

Figure 8. **BAI** 12.5 mM; SmI_2 1.25 mM; TFE 25 mM; (A) HMPA 0 mM; (B) HMPA 0.5 mM; (C) HMPA 1.1 mM; (D) HMPA 2.0 mM.

delayed as the concentration of the HMPA increases. However, after a transition period, at 8 mM HPMA, the fit to a first order is very good (Figure 9).

The rate constants increase as the concentration of the HMPA further increases. For HMPA concentrations of 8, 16, and 32 mM, the first-order rate constants are 1.8, 3.7, and 10.3 s^{-1}, respectively. Thus, at low concentrations, the HMPA slows the reaction by preventing the formation of the solid and hence catalytic sites. However, at higher concentrations, it enhances the reactions, probably due to the increase in the reduction potential of SmI_2.[7]

It is difficult to say, based on the present information, what would have been the nature of the reaction if the catalytic surfaces would have not been formed in the course of the reaction. It is possible that the reaction could enjoy catalysis by individual SmI_3 molecules acting as Lewis acids. Such catalysis is well documented in the literature as having synthetic importance.[4a,9] As we can see from Figure 8, the time to completion of the reaction becomes longer as the concentration of the HMPA increases. This may indicate that HMPA interferes with crystal formation, thus preventing the surface catalysis. However, it may also indicate that HMPA prevents individual SmI_3 molecules from coordinating to the substrate and enhancing the reaction. Another possibility is that the HMPA prevents the coordination of SmI_2 to the lone pair of the imine.

We recall that the data produced with MeOH were not very conclusive regarding the rates. This is demonstrated in the reaction of SmI_2 = 1.25 mM, imine = 12.5 mM with various concentrations of MeOH. Table 2 shows the initial slopes for the reactions in the absence and in the presence of SmI_3.

There are several points that are worth noting. The rate is enhanced when SmI_3 is added to the reaction mixture. In all cases, the rate goes up from 0.1 to 0.5 M MeOH and then decreases upon going to 4 M of MeOH. The dependence on the concentration of SmI_3 is relatively weak and is more pronounced at the lower concentrations of MeOH. The effect of MeOH can be easily understood on the basis of its ability to complex SmI_2.[3a,c] On the one hand, the complexation may enhance the reaction by

rendering the protonation of the radical anion a unimolecular process within an ion pair. On the other hand, at high MeOH concentrations, it coordinates more effectively to the SmI_2, preventing its docking on the surface, and at the same time it may also interfere with the crystal formation of the SmI_3. These opposing effects are probably the cause of the observed weak rate dependence on the MeOH concentration.

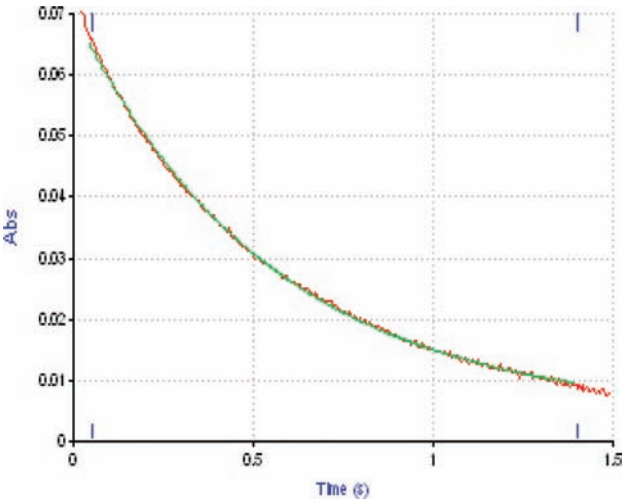

Figure 9. **BAI** 12.5 mM; SmI_2 1.25 mM; TFE 25 mM; HMPA = 8.0 mM; $k = 1.8\ s^{-1}$.

Table 2. Effect of SmI_3 and MeOH on the Reaction Rates of BAI (12.5 mM) and SmI_2 (1.25 mM)

$[SmI_3]$, M	[MeOH], M	−slope, abs/s
0	0.1	0.004
	0.5	0.06
	4	0.04
1.25	0.1	0.13
	0.5	0.34
	4	0.25
2.5	0.1	0.18
	0.5	0.52
	4	0.33
5.0	0.1	0.23
	0.5	0.55
	4	0.32

We can sum the mechanism by which the imine undergoes catalytic reduction as follows. In the course of the reaction, the divalent samarium is converted to a trivalent one, which forms microcrystals. Sites on the surface of these microcrystals may host SmI_2 and increase its reactivity toward the imine, whose reaction is first order. The first-order kinetics in the TFE may suggest that the protonation either takes place prior to, or is, the rate-determining step. We believe that the role of TFE is to protonate the radical anion. After protonation of the radical anion, the formed alkoxide binds itself to the trivalent samarium and removes it from the active site, enabling a new SmI_2 to occupy this site (see Scheme 1).

The picture presented above seems to describe the mechanism of the reaction reasonably well. However, there are a few fine-tuning questions that cannot be fully answered at this stage. For example, does the SmI_2 retain its identity as the reducing entity, or, following an internal electron transfer (eq 2), does another molecule take the role of the reducing agent?

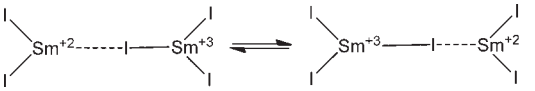

(2)

Other interesting questions are as follows: What are the kinetics of the microcrystals formation as well as their aggregation and homogeneity? Are the microcrystals made of pure SmI_3 obtained via the equilibrium (eq 3):

$$2SmI_2(OR) \rightleftharpoons SmI_3 + SmI(OR)_2 \qquad (3)$$

or are they a mixture of Sm^{3+} with a variety of ligands? At this point, the answer to these and other questions will have to await further studies.

Over the years, the kinetics of the reactions of SmI_2 with many substrates has been studied. To the best of our knowledge, such a unique case of surface catalysis has never been encountered before. This clearly indicates that the catalytic effect is substrate dependent. The question is whether this phenomenon of auto/surface catalysis observed with the present substrate is a singular point in the space of SmI_2 reactions or is it general within the imine family? To answer this, we examined two other imines, *N*-benzylidenemethylamine (**BMI**) and benzophenonimine (**BPI**). In both cases, we used the effect of HMPA as our diagnostic tool. Four kinetic traces of the reaction of **BMI** with SmI_2 in the presence of HMPA are shown in Figure 10.

The reactions are very fast as compared to the **BAI**. In the absence of HMPA, the half-life of the reaction is less than 10 ms, and in the presence of 32 mM of HMPA, the half-life increases

Scheme 1

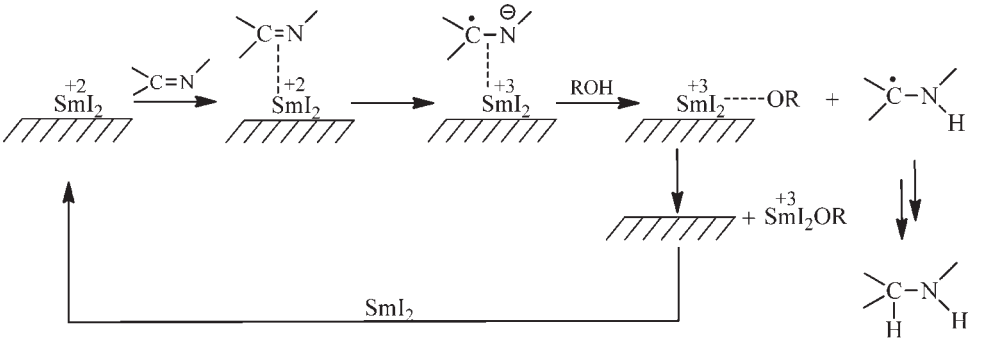

dx.doi.org/10.1021/ja205885q |*J. Am. Chem. Soc.* 2011, 133, 14795–14803

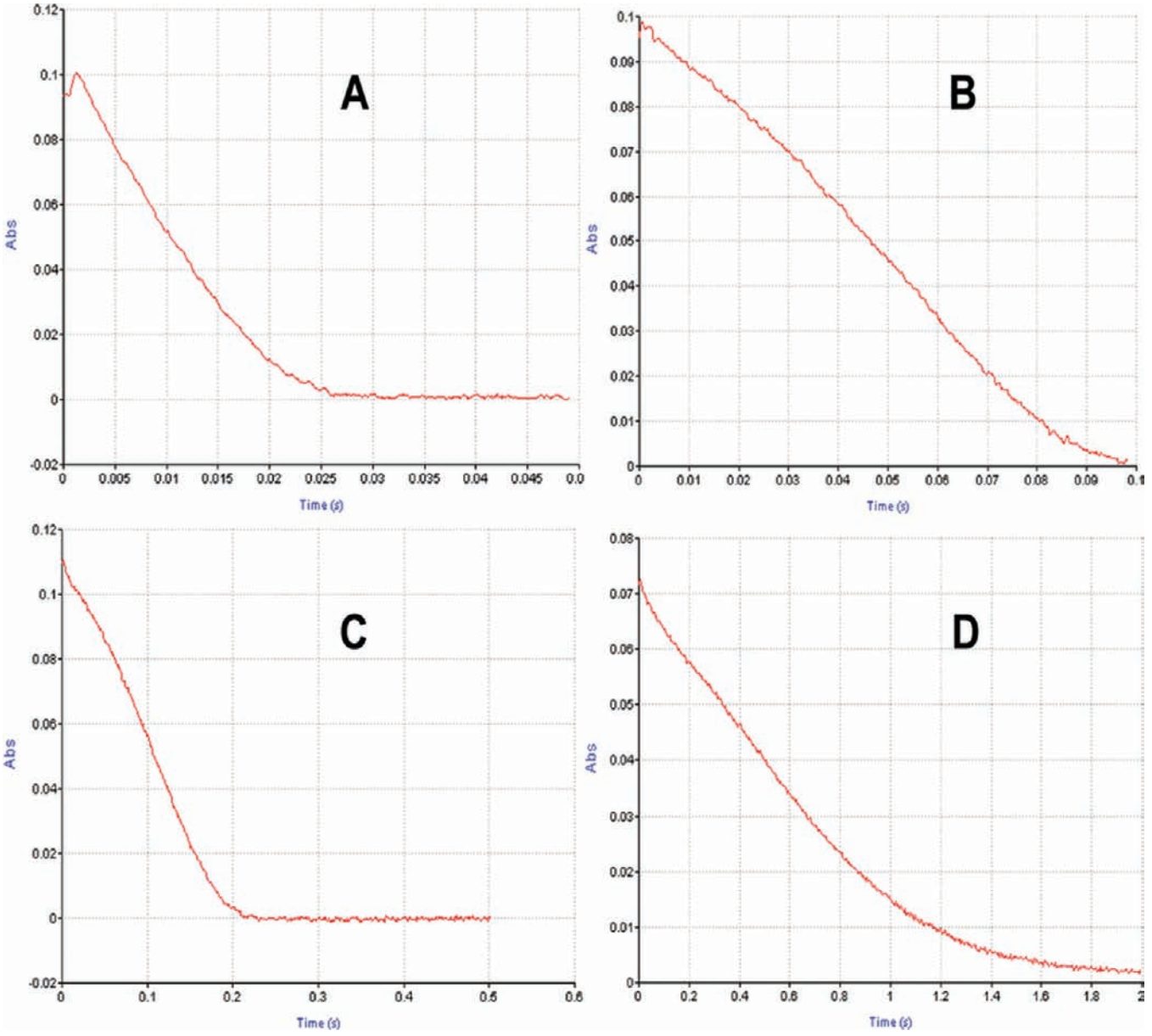

Figure 10. **BMI** 12.5 mM; SmI_2 1.25 mM; TFE 25 mM; (A) HMPA 0 mM; (B) HMPA 1.1 mM; (C) HMPA 2.0 mM; (D) HMPA 32 mM.

to ca. 600 ms. The structure of the kinetic trace becomes more "normal" as the concentration of HMPA increases, but does not reach the stage of a pure first order. Nevertheless, it clearly shows that this imine-like **BAI** also displays an autocatalytic behavior.

The fastest of the three imines is the **BPI**. In the absence of HMPA, its reaction is nearly completed in the dead time of the instrument. Yet, the autocatalytic behavior is clearly recognizable (Figure 11). Again, as the concentration of HMPA increases along the series 0.0, 0.5, 2, and 2.5 mM, the half-lives increase as well (2.3, 6.5, 37, 40 ms, respectively). At 4 mM HMPA, the kinetics convert to a classical first-order reaction, Figure 11E, with slightly decreasing rate constants 3.9, 3.2, and 2.6 s^{-1} for 4, 8, and 16 mM HMPA.

The fact that all three imines display the same autocatalytic behavior suggests that this behavior is typical of the reactions of imines with SmI_2.

The various observations made in this study have enabled us to learn about the reaction mechanism of the imines beyond the phenomenon of the autocatalysis. We note that the order of reactivity is **BPI** > **BMI** > **BAI**. We note also that the effect of HMPA on the rate is different for the different substrates. The reaction rate of all three substrates decreases as the HMPA concentration increases up to 4 mM. For **BAI**, a further increase in the HMPA concentration induces rate enhancement. For the **BMI**, rate retardation continues, whereas for **BPI** there is a very moderate depression of the rate. Let us begin with the reactivity order. We have performed ab initio calculations at the B3LYP/6-31+G* level using the Gaussian suite of programs[10] including THF as the solvent using the Onsager model (see the Supporting Information). The order of the electron affinity measured as the energy difference between the radical anion and the neutral relative to **BMI** is (numbers in parentheses are in kcal/mol):

$$\textbf{BAI}\ (-11.86) > \textbf{BPI}\ (-5.72) > \textbf{BMI}\ (0)$$

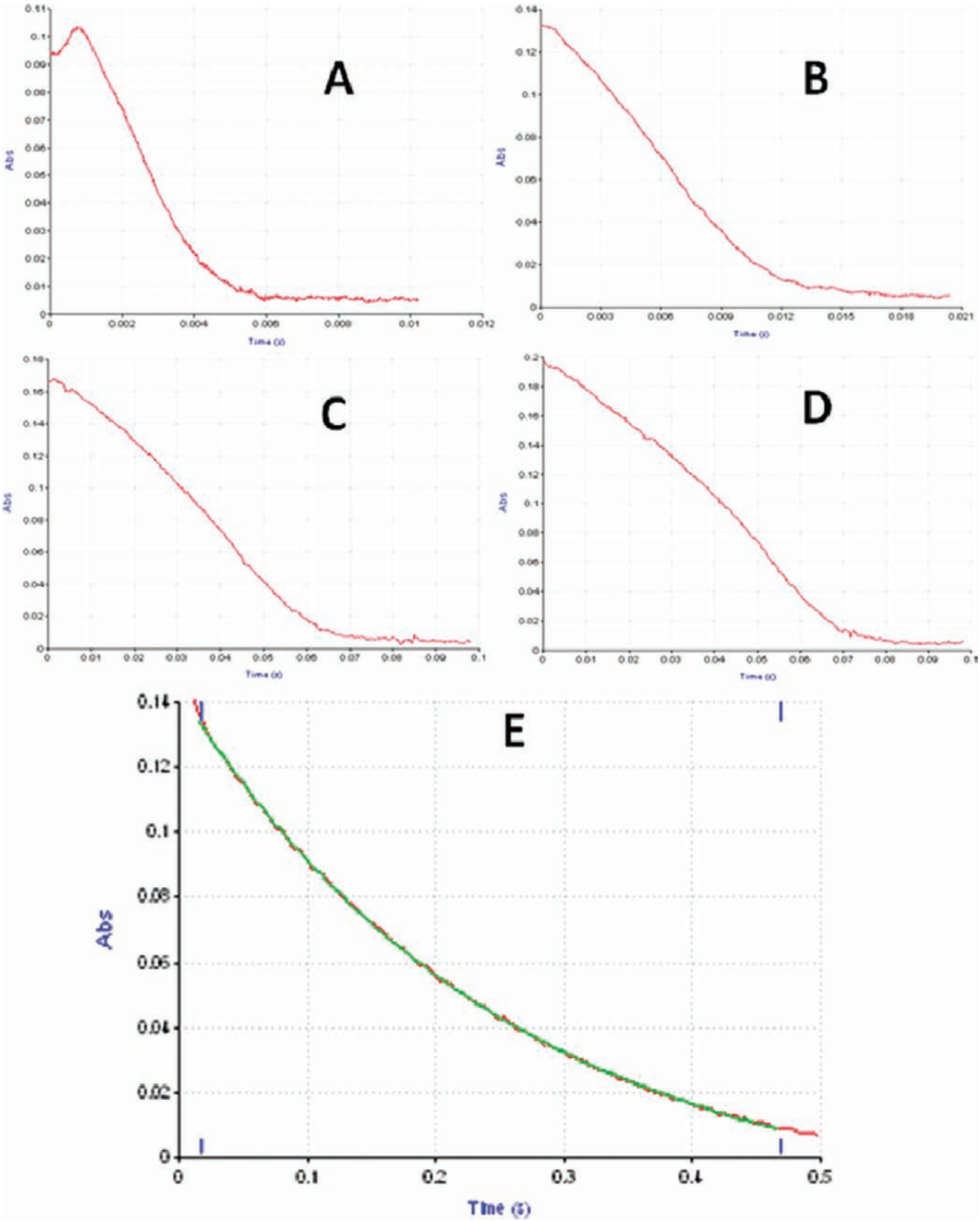

Figure 11. **BPI** 12.5 mM; SmI_2 1.25 mM; TFE 25 mM; (A) HMPA 0 mM; (B) HMPA 0.5 mM; (C) HMPA 2.0 mM; (D) HMPA 2.5 mM; (E) HMPA 4 mM.

Thus, the substrate with the highest electron affinity (**BAI**) is the slowest to react. We note, however, that the reactivity order follows closely the accessibility to the nitrogen lone pair. The least-hindered substrate is **BPI**, and undoubtedly the steric

crowding by the anilino phenyl group in **BAI** is much larger than that of the methyl group in **BMI**. Thus, it seems clear that for an effective reaction the samarium has to coordinate to the lone pair of the nitrogen. Most probably the coordination is to Sm^{2+}, although in the surface catalysis mode it could be to a neighboring trivalent samarium ion. This model fits nicely the observed HMPA effect. Parallel to the surface catalytic reaction, a direct reaction between the SmI_2 and the substrates may also exist. This inner sphere electron transfer[11] is very fast and definitely plays an important role in the early stages of the reaction before enough Sm^{3+} is generated to commence the surface catalysis. At certain concentrations of HMPA, the surface catalysis is quenched, and two reaction paths remain open, one through the direct coordination of the SmI_2 to the nitrogen lone pair, and the other is an outer sphere mechanism that benefits from the higher reduction potential of the HMPA−SmI_2 complex. In the case of **BAI**, where the direct coordination is considerably hindered, the coordination of SmI_2 by the HMPA will enhance the reaction. On the other hand, for the two other substrates, **BPI** and **BMI**, the precoordination of the SmI_2 to the substrate is more effective than the HMPA−SmI_2 complex mechanism. Therefore, rate retardation is caused by the further reduction of the small amounts of free or partial HMPA-coordinated SmI_2.

SUMMARY AND CONCLUSIONS

The three imines studied with SmI_2 in THF all featured the same autocatalytic behavior, suggesting autocatalysis to be a general feature for imino substrates. After SmI_2 transfers an electron to the substrate, it becomes trivalent samarium, whose salt is sparingly soluble in THF. Although no solids are visible to the naked eye, the existence of microcrystals was proven by light microscopy as well as by dynamic light scattering analysis. It turns out that catalytic sites exist on the surface of the solid. Therefore, as the reaction progresses, more of these catalytic sites are formed, causing an autocatalytic reaction profile.

In addition, it was found that the reactivity order of the three imines does not correlate with their electron affinity, as is common in the chemistry of SmI_2, but rather with the steric accessibility to the nitrogen lone pair. Thus, in the noncatalytic reaction, the SmI_2 coordinates first to the nitrogen lone pair, leading to a very efficient inner sphere electron transfer process. As a natural continuation, we have initiated a study with substrates where the binding site does not coincide with the reaction site, such as in pyridine derivatives.

EXPERIMENTAL SECTION

General. THF was dried and freshly distilled over Na wire and benzophenone under argon atmosphere. TFE and MeOH were dried according to known procedures.[12] Water content was determined and found to be lower than 20 ppm. SmI_2 was diluted as needed from a 0.1 M freshly prepared THF solution.[13] The concentration of the SmI_2 solution was spectroscopically determined (λ = 619 nm; ε = 635). The imines **BAI**, **BMI**, and **BPI** are commercially available and were distilled before use. The product structures were confirmed by comparing their ^{1}H (600 or 300 MHz) and ^{13}C (150 or 75 MHz) NMR spectra and the HRMS data with literature values.[5j,14,15]

Kinetics. The kinetics of the reactions were followed using a stopped flow spectrophotometer in a glovebox under nitrogen atmosphere at room temperature. The flow system was cleaned with 1 N HCl before conducting a series of kinetic experiments to ensure that no catalytic solids remain in the system. The reactions were monitored at the λ_{max} of the SmI_2 (619 nm). Whenever proton donor was used, the proton donor was mixed with the substrate solution. Each set of experiments was repeated two to three times. Within a set, each measurement was routinely repeated three times. At the end of each series, the first measurement was repeated to ensure reproducibility within a set. The deviation usually observed less than 5%. First-order kinetics were analyzed using Kinet Asyst (v. 2.2 Hi-Tech Ltd.).

General Procedure for Product Preparation under Conditions Similar to the Kinetic Measurements. A freshly prepared solution of SmI_2 (0.1 M) in THF was added in the glovebox to a homogeneous solution of the imine and TFE in dry THF. The total volume of the reaction was 200 mL. The final concentrations were [SmI_2] = 2.5 mM, [imine] = 1 mM, and [TFE] = 0.1 M. After 5 min, the solvent was evaporated under reduced pressure at 30 °C. The crude reaction mixture was redissolved in DCM (50 mL), washed consecutively with solutions of saturated $NaHCO_3$ (10 mL), saturated $Na_2S_2O_3$ (10 mL), potassium dihydrogen phosphate buffer (20 mL), followed by brine (20 mL), and dried over anhydrous Na_2SO_4. The solvent was evaporated under reduced pressure. Under these conditions, **BAI** gave 25% reduced product and 75% of the coupled product. The two other imines gave only coupled products.

Preparation of SmI_3 Solution in THF. To the homogeneous solution of SmI_2 in THF was added a freshly prepared I_2 solution in THF. The concentration of I_2 was one-half that of the SmI_2. The freshly prepared yellowish-green solution of SmI_3 in THF was used for the kinetic experiments as well as dynamic light scattering, light microscopy, and HRTEM analyses.

ASSOCIATED CONTENT

Supporting Information. Complete ref 10, light microscopy of SmI_3 with various filters, dynamic light scattering measurement figures, kinetic traces of the reaction of **BAI** and SmI_2 in the presence of MeOH, HRTEM of SmI_3, and Gaussian archives for the computed structures. This material is available free of charge via the Internet at http://pubs.acs.org.

AUTHOR INFORMATION

Corresponding Author
shoz@mail.biu.ac.il

ACKNOWLEDGMENT

We thank Dr. J. Grinblat for the HRTEM analysis.

REFERENCES

(1) (a) Matignon, C. A.; Caze, E. *Ann. Chim. Phys.* **1906**, *8*, 417–426. (b) Namy, J. L.; Girard, P.; Kagan, H. B. *New J. Chem.* **1977**, *1*, 5–7. For review, see:(c) Kagan, H. B. *Tetrahedron* **2003**, *59*, 10351–10372. (d) Molander, G. A. *Chem. Rev.* **1992**, *92*, 29–60. (e) Molander, G. A.; Harris, C. R. *Chem. Rev.* **1996**, *96*, 307–338. (f) Molander, G. A.; Harris, C. H. *Tetrahedron* **1998**, *54*, 3321–3354. (g) Nicolaou, K. C.; Ellery, S. P.; Chen, J. S. *Angew. Chem., Int. Ed.* **2009**, *48*, 7140–7165. (h) Krief, A.; Laval, A.-M. *Chem. Rev.* **1999**, *99*, 745–777. (i) Gansäuer, A.; Bluhm, H. *Chem. Rev.* **2000**, *100*, 2771–2788. (j) Nakata, T. *Chem. Soc. Rev.* **2010**, *39*, 1955–1972. (k) Ichikawa, S. *Chem. Pharm. Bull.* **2008**, *56*, 1059–1072. (l) Soderquist, J. A. *Aldrichimica Acta* **1991**, *24*, 15–23. (m) Concellón, J. M.; Rodríguez-Solla, H.; Concellón, C.; Amo, V. *Chem. Soc. Rev.* **2010**, *39*, 4103–4113. (n) Edmonds, D. J.; Johnston, D.; Procter, D. J. *Chem. Rev.* **2004**, *104*, 3371–3403.(o) Procter, D. J.; Flowers, R. A., II; Skrydstrup, T. *Organic Synthesis Using Samarium Diiodide: A Practical Guide*; The Royal Society of Chemistry: Cambridge, UK, 2010.

(2) (a) Flowers, R. A., II. *Synlett* **2008**, *10*, 1427–1439. (b) Dahlén, A.; Hilmersson, G. *Eur. J. Inorg. Chem.* **2004**, 3393–3403.

(3) (a) Amiel-Levy, M.; Hoz, S. *J. Am. Chem. Soc.* **2009**, *131*, 8280–8284. (b) Tarnopolsky, A.; Hoz, S. *Org. Biomol. Chem.* **2007**, *5*, 3801–3804. (c) Tarnopolsky, A.; Hoz, S. *J. Am. Chem. Soc.* **2007**, *129*, 3402–3407. (d) Yacovan, A.; Hoz, S. *J. Org. Chem.* **1997**, *62*, 771–772. (e) Yacovan, A.; Bilkis, I.; Hoz, S. *J. Am. Chem. Soc.* **1996**, *118*, 261–262.

(4) (a) Farran, H.; Hoz, S. *J. Org. Chem.* **2009**, *74*, 2075–2079. (b) Farran, H.; Hoz, S. *Org. Lett.* **2008**, *10*, 4875–4877. (c) Farran, H.; Hoz, S. *Org. Lett.* **2008**, *10*, 865–867. (d) Kleiner, G.; Tarnopolsky, A.; Hoz, S. *Org. Lett.* **2005**, *7*, 4197–4200.

(5) (a) Enholm, E. J.; Forbes, D. C.; Holub, D. P. *Synth. Commun.* **1990**, *20*, 981–987. (b) Imamoto, T.; Nishimura, S. *Chem. Lett.* **1990**, 1141–1142. (c) Machrouhi, F.; Namy, J.-L. *Tetrahedron Lett.* **1999**, *40*, 1315–1318. (d) Annunziata, R.; Benaglia, M.; Cinquini, M.; Cozzi, F.; Raimondi, L. *Tetrahedron Lett.* **1998**, *39*, 3333–3336. (e) Collin, J.; Giuseppone, N.; Machrouhi, F.; Namy, J.-L.; Nief, F. *Tetrahedron Lett.* **1999**, *40*, 3161–3164. (f) Lebrun, A.; Rantze, E.; Namy, J.-L.; Kagan, H. B. *New J. Chem.* **1995**, *19*, 699–705. (g) Banik, B. K.; Zegrocka, O.; Banik, I.; Hackfeld, L.; Becker, F. F. *Tetrahedron Lett.* **1999**, *40*, 6731–6734. (h) Kim, M.; Knettle, B. W.; Dahlén, A.; Hilmerssonb, G.; Flowers, R. A., II. *Tetrahedron* **2003**, *59*, 10397–10402. (i) Dahlén, A.; Prasad, E.; Flowers, R. A., II; Hilmersson, G. *Chem.-Eur. J.* **2005**, *11*, 3279–3284. (j) Dahlén, A.; Hilmersson, G. *Chem.-Eur. J.* **2003**, *9*, 1123–1128.

(6) Atkins, P. W. *Physical Chemistry*, 4th ed.; Oxford University Press: Oxford, UK, 1990.

(7) Shabangi, M.; Flowers, R. A., II. *Tetrahedron Lett.* **1997**, *38*, 1137–1140.

(8) At the very early beginning of the trace, there is a short part of "normal" behavior. This is usually attributed to the reaction of the trace amount of water, which is manifested only when proton donor concentration is very low. At higher concentrations of alcohol, this phenomenon disappears, apparently because the interaction of molar concentrations of the proton donor with the water largely exceeds the water interaction with the SmI_2.

(9) (a) Coote, S. C.; Quenum, S.; Procter, D. J. *Org. Biomol. Chem.* **2011**, *9*, 5104–5108. (b) Evans, D. A.; Hoveyda, A. H. *J. Am. Chem. Soc.* **1990**, *112*, 6447–6449.

(10) Frisch, M. J.; et al. *Gaussian 03*, revision A.04; Gaussian, Inc.: Pittsburgh, PA, 2003. (For complete references, see the Supporting Information.)

(11) (a) Ankner, T.; Hilmersson, G. *Tetrahedron* **2009**, *65*, 10856–10862. (b) Enemærke, R. J.; Daasbjerg, K.; Skrydstrup, T. *Chem. Commun.* **1999**, 343–344. (c) Prasad, E.; Flowers, R. A., II. *J. Am. Chem. Soc.* **2002**, *124*, 6895–6899. (d) Enemærke, R. J.; Hertz, T.; Skrydstrup, T.; Daasbjerg, K. *Chem.-Eur. J.* **2000**, *6*, 3747–3754. (e) Shabangi, M.; Kuhlman, M. L.; Flowers, R. A., II. *Org. Lett.* **1999**, *1*, 2133–2135. (f) Prasad, E.; Knettle, B. W.; Flowers, R. A., II. *J. Am. Chem. Soc.* **2002**, *126*, 6891–6894. (g) Miller, R. S.; Sealy, J. M.; Shabangi, M.; Kuhlman, M. L.; Fuchs, J. R.; Flowers, R. A., II. *J. Am. Chem. Soc.* **2000**, *122*, 7718–7722.

(12) Perrin, D. D.; Armarego, W. L. F. *Purification of Laboratory Chemicals*, 3rd ed.; Pergamon Press: New York, 1989.

(13) Girard, P.; Namy, J. L.; Kagan, H. B. *J. Am. Chem. Soc.* **1980**, *102*, 2693–2698.

(14) Winn, M.; Dunnigan, D. A.; Zaugg, H. E. *J. Org. Chem.* **1968**, *33*, 2388–2302.

(15) Mikolaj, J.; Maciej, U.; Irena, K.-S.; Mieczyslaw, M. *Pol. J. Chem.* **1981**, *55*, 1309–1320.